Design and Fabrication of Passive Wireless SAW Sensor for Pressure Measurement

Shuhei Hashimoto Non-member (Nissan Motor Co.,Ltd , shuhei-h@mail.nissan.co.jp)
Jan H. Kuypers Non-member (Tohoku University, jan@mems.mech.tohoku.ac.jp)
Shuji Tanaka Member (Tohoku University, shuji@cc.mech.tohoku.ac.jp)
Masayoshi Esashi Member (Tohoku University, esashi@cc.mech.tohoku.ac.jp)

Keywords : wireless sensor, surface acoustic wave (SAW), SAW delay line, pressure sensor, hermetic sealing, lithium niobate ($LiNbO_3$)

It is important for current automobiles to measure various physical values such as stress, temperature, pressure and acceleration in use as well as in the development. Surface acoustic wave (SAW) sensors have the advantage of being able to measure several physical values such as stress, temperature and pressure without battery and wires. In this paper, we focus on pressure measurement, which is necessary for engines, tires and car bodies.

The structure of our SAW pressure sensor is shown in Figure 1. We use 128° YX $LiNbO_3$, which is a piezoelectric single crystal often used for SAW devices, as a substrate material. This substrate has a high coupling coefficient of 5.5 % for SAW propagating in X direction, and does not generate an unwanted bulk wave. In addition, the substrate has a low SAW propagation loss of 5~6 dB/μs. From these features, 128 ° YX $LiNbO_3$ is suitable for passive SAW sensors.

As shown in Figure 1, the sensor has one IDT and four reflectors. A SAW generated by the IDT propagates in both directions, reflects at the reflectors, and then returns to the IDT after time delay τ_n (n = 1~4 for the reflector 1~4). The pressure-detective diaphragm is placed between the reflectors 3 and 4, and the responses of the reflectors 3 and 4 are used for pressure measurement. The reflectors 1 and 2 serve as temperature compensation. If the temperature of the sensor changes, the reflector responses considerably change, because 128° YX $LiNbO_3$ has a large TCD (temperature coefficient of time delay) of 71.2 ppm/K. Therefore, the temperature compensation, which is realized by the reflectors 1 and 2, is essential. The pitch of the IDT and the reflectors is 400 nm, which is one forth of the wavelength, for the excitation of 2.45 GHz SAW.

The SAW delay line sensor is patterned on a 100 μm thick 128° YX $LiNbO_3$ substrate using a electron beam lithography system. Figure 2 shows a fabricated IDT. Hermetic bonding of the first and second layers is necessary to form the reference pressure cavity. In this study, we selected direct bonding in air, because it needs no intermediate layer, which can degrade the temperature characteristic of the sensor.

The relationship between applied pressure and the phase change of the SAW pressure sensor was measured. In the depressurization from 280 kPa to 20 kPa, the phase φ_4 ($\varphi_n = 2\pi f\tau_n$) corresponding to the reflector 4 largely changed according to the pressure change, while the change of the other phases were smaller. The pressure is estimated with temperature compensation using the following effective phase:

$$\varphi_{\mathrm{eff}} = \varphi_4 - \varphi_3 - \frac{d-c}{b-a}(\varphi_2 - \varphi_1) \quad \cdots\cdots (1)$$

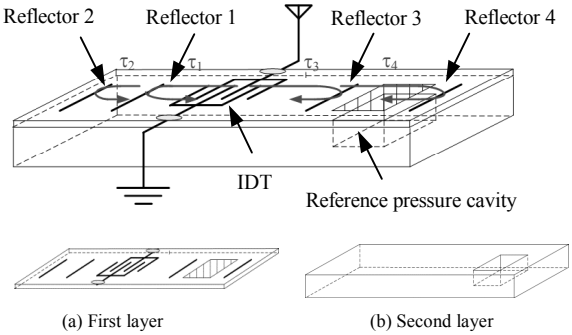

Fig. 1. Schematic structure of the SAW delay line pressure sensor

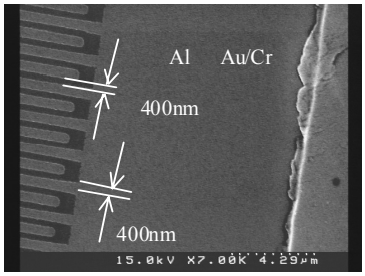

Fig. 2. Fabricated interdigital transducer

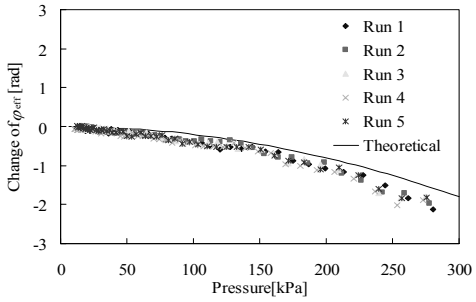

Fig. 3. Change of the effective phase φ_{eff} by pressure change

where a, b, c and d are the length of the delay lines 1, 2, 3 and 4, respectively. Figure 3 shows the effective phase φ_{eff} as a function of the pressure for five runs. The result shows good repeatability, suggesting pressure measurement based φ_{eff} is feasible. The obtained φ_{eff} is nearly similar to the theoretical estimation.

Finally, the influence of a tire on the wireless interrogation of the sensor was investigated. The result indicates that automobile tires have little negative influence on wireless communication, at least if they do not rotate.

Paper

Design and Fabrication of Passive Wireless SAW Sensor for Pressure Measurement

Shuhei Hashimoto* Non-member
Jan H. Kuypers** Non-member
Shuji Tanaka** Member
Masayoshi Esashi*** Member

This paper mainly presents the design and fabrication of a TDMA (time division multiple access) passive wireless pressure sensor using 2.45 GHz surface acoustic wave (SAW) delay lines. The SAW pressure sensor consists of two $LiNbO_3$ substrates. The first layer is a pressure-detective thin substrate, on which an interdigital transducer (IDT) and reflectors are fabricated. The second layer is a support substrate, in which a reference pressure cavity is etched. These two substrates are directly bonded. The pressure measurement was successfully demonstrated in a pressure range of 20~280 kPa with good repeatability. In addition, the influence of a tire on the wireless interrogation of the sensor was investigated. Automobile tires have little negative influence on wireless communication, at least if they do not rotate.

Keywords : wireless sensor, surface acoustic wave (SAW), SAW delay line, pressure sensor, hermetic sealing, lithium niobate ($LiNbO_3$)

1. Introduction

It is important for current automobiles to measure various physical values such as stress, temperature, pressure and acceleration in use as well as in the development. To measure the physical values of rotating parts such as tires, drive shafts and steering shafts, wireless sensors are preferred. In addition, the mass of the sensor must be as small as possible, because it has a large impact on the rotation balance. Particularly, the weight of a battery occupies several ten percentages of the total weight of active wireless sensors. The recharging or replacement of empty batteries is also a problem.

Surface acoustic wave (SAW) sensors have the advantage of being able to measure several physical values such as stress, temperature and pressure without battery[(1)(2)]. In this paper, we focus on pressure measurement, which is necessary for engines, tires and car bodies. To date, pressure sensors using SAW have been reported[(3)(4)]. There are typically two types of sensor: SAW delay line sensor and SAW resonator sensor[(1)(2)].

The SAW resonator sensor can realize multiple access by frequency division, and the number of simultaneously-accessible sensors can be increased within an available bandwidth. The resolution of the sensor depends on Q values, i.e. a higher Q value leads to higher resolution. The SAW delay line sensor can also realize multiple access by time division. The number of simultaneously-accessible sensors is determined by the longest delay line, whose length is limited by the attenuation of the SAW (e.g. 5~6 dB/μs at 2.45GHz for 128° YX $LiNbO_3$[(5)]). We successfully interrogated four SAW temperature sensors by time division multiple access (TDMA) at 2.45 GHz[(6)]. The resolution of the sensor is also determined by the length of delay lines.

We need sensors as small as possible from the abovementioned reason. To make the sensor smaller, a higher frequency is preferable, because the antenna can be made smaller. Among the available RF bands, we selected ISM band at 2.45 GHz, where the length of the antenna can be reduced to several centimeters.

The Q value of SAW resonators, that is, the resolution of the SAW resonator sensors generally drops with increase in frequency. Contrarily, the phase sensitivity of the SAW delay line sensors, which is proportional to the product of the frequency and time delay, rises with increase in frequency. At 2.45 GHz, the SAW delay line sensors have advantage in the resolution in comparison with the SAW resonator sensors. Thus, we developed a pressure sensor using SAW delay lines in this study. The disadvantage of the SAW delay line sensors based on TDMA is the limited number of simultaneously-accessible sensors, which is practically less than 10[(7)].

In this paper, the design of the pressure sensor, including the diaphragm, an interdigital transducer (IDT) and reflectors, is first described. Next, the fabrication technology of the pressure sensor is presented. Finally, pressure sensing results are described.

2. Design of SAW Pressure Sensor

The structure of our SAW pressure sensor is shown in Figure 1. We use 128° YX $LiNbO_3$, which is a piezoelectric single crystal often used for SAW devices, as a substrate material. This substrate has a high coupling coefficient of 5.5 % for SAW propagating in X direction, and does not generate an unwanted bulk wave. In addition, the substrate has a low SAW propagation loss of 5~6 dB/μs at 2.45GHz[(5)]. From these features, 128° YX $LiNbO_3$ is suitable for passive SAW sensors.

The SAW pressure sensor consists of two parts: The first layer is a pressure-detective thin substrate, on which an IDT and reflectors are fabricated. The second layer is a support substrate, in

* Measurement Engineering Department, Nissan Motor Co., Ltd.
560-2 Okatsukoku, Atsugi, Kanagawa 243-0192
** Department of Nanomechanics, Tohoku University
6-6-01 Aza Aoba, Aramaki, Sendai, Miyagi 980-8579
*** Micro/Nano Machining Research and Education Center, Tohoku University
6-6-01 Aza Aoba, Aramaki, Sendai, Miyagi 980-8579

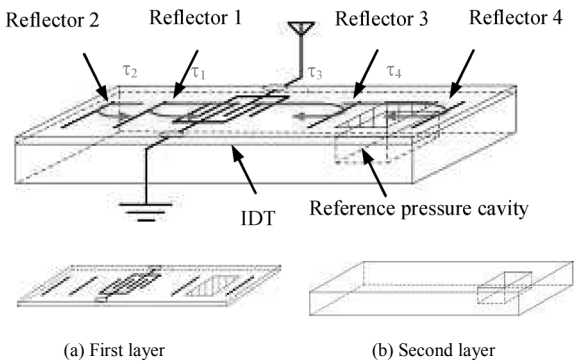

(a) First layer (b) Second layer

Fig. 1. Schematic structure of the SAW delay line pressure sensor

Table 1. Designs of the IDT and the reflectors

	Number	Pitch	Length	Thickness	Material
IDT	27	395 nm	127 μm	100 nm	Al
Reflector 1 and 3	11	401 nm	127 μm	100 nm	Al
Reflector 2 and 4	61	401 nm	127 μm	100 nm	Al

which a reference pressure cavity is made. These two wafers are hermetically bonded. Reference[8] reported a pressure sensor working on a similar principle, but the hermetic sealing of the reference pressure cavity was not achieved.

As shown in Figure 1, the sensor has one IDT and four reflectors. A SAW generated by the IDT propagates in both directions, reflects at the reflectors, and then returns to the IDT after time delay τ_n (n = 1~4 for the reflector 1~4). The pressure-detective diaphragm is placed between the reflectors 3 and 4, and the responses of the reflectors 3 and 4 are used for pressure measurement. The reflectors 1 and 2 serve as temperature compensation. The pitch of the IDT and the reflectors is 400 nm, which is one forth of the wavelength, for the excitation of 2.45 GHz SAW. The number of the electrodes of the reflectors 1 and 3 is 11 for a reflectivity of 50 %, and that of the reflectors 2 and 4 is 61 for a reflectivity of 99.9%. The detail designs of the IDT and the reflectors are shown in Table 1.

The change of time delay for the reflector 4 by pressure change is caused by the stretch of the diaphragm section as a SAW propagation path. The strain-dependant formulation of time delay τ_4 is represented as

$$\tau_4(\varepsilon) = \tau_0(1 + SCD \cdot \varepsilon) \quad \text{and} \cdots\cdots (1)$$

$$SCD = \frac{1}{\tau_4}\frac{\partial \tau_4}{\partial \varepsilon} = \frac{1}{l}\frac{\partial l}{\partial \varepsilon} - \frac{1}{v}\frac{\partial v}{\partial \varepsilon} = 1 - \frac{1}{v}\frac{\partial v}{\partial \varepsilon}, \cdots\cdots (2)$$

where ε is strain, τ_0 is the initial time delay, v is SAW propagation velocity, and l is the length of the SAW propagation path (round trip). For 128° YX $LiNbO_3$, *SCD* (strain coefficient of time delay) is theoretically 1, since $\partial v/\partial \varepsilon = 0$. In other words, τ depends only on the variance of l induced by diaphragm deformation under constant temperature condition[9]. If the temperature of the sensor changes, the reflector responses considerably change, because 128° YX $LiNbO_3$ has a large *TCD* (temperature coefficient of time delay) of 72 ppm/K[10]. Therefore, the temperature compensation, which is realized by the reflectors 1 and 2, is essential.

Our SAW wireless pressure sensor is designed to operate in the pressure range from 0 kPa to 600 kPa. The size of the reference pressure cavity is designed from the theoretical calculation of clamped rectangular plates. The deflection of the diaphragm by pressure is calculated using the following equation[11]:

$$\frac{\partial^4 w}{\partial x^4} + 2\frac{\partial^4 w}{\partial^2 x \partial^2 y} + \frac{\partial^4 w}{\partial y^4} = \frac{p}{D}, \cdots\cdots (3)$$

where w is the deflection of the diaphragm, p is the pressure, and D is the bending stiffness. The stretch of the diaphragm section is calculated from the distribution of w over the diaphragm, and the time delay $\tau_4(\varepsilon)$ is obtained from Equations (1) and (2).

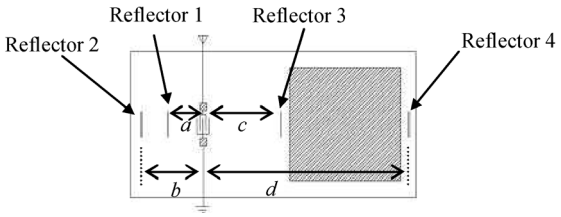

a = 1.33 mm, b = 2.0 mm, c = 3.4 mm, d = 9.0 mm

Fig. 2. Design of the SAW pressure sensor

In this study, the designed size of the diaphragm is 5.4 mm square and 100 μm in thickness. In this case, the maximum deflection of the diaphragm at 600 kPa is approximately 40 μm, which gives the minimum required depth of the reference pressure cavity. Finally, we determined the position of each reflector, as shown in Figure 2. The initial τ_1, τ_2, τ_3 and τ_4 are 0.695 μs, 1.031 μs, 1.705 μs and 4.594μs, respectively, when SAW propagation velocity is 3979 m/s.

3. Fabrication Process

3.1 IDT and Reflectors The SAW delay line sensor is patterned on a chemically-reduced 100 μm thick 128° YX $LiNbO_3$ substrate using an electron beam lithography system (JEOL, JBX-5000LS). The patterns of the IDT and the reflectors are formed by patterning 400 nm thick positive type electron beam (EB) resist (ZEON, ZEP520A) with a dose of 88 μC/cm^2 at a beam current of 100 pA and an acceleration voltage of 50 kV. Subsequently, 100 nm thick Al is deposited by electron beam evaporation, and then lifted off. The bond pads are formed by another lift-off step of 10 nm thick Cr and 300 nm thick Au using image reversal photoresist (Clariant, AZ5214E). EB resist (ZEON, ZEP520A) is used as a buffer layer to prevent Al etching by photoresit developer, and plasma-etched before Al evaporation. Figure 3 shows a fabricated IDT.

3.2 Reference Pressure Cavity The cavity is fabricated in a chemically-reduced 500 μm thick 128° YX $LiNbO_3$ substrate. We tried two fabrication methods: wet etching and sandblast. For wet etching, a Au/Cr mask is formed by sputtering and wet etching on the surface toward − z direction, because $LiNbO_3$ is preferentially etched on the −z face. The masked substrate is etched in HF at 80°C, as reported previously[12]. Figure 4 (a) shows a 40 μm deep cavity fabricated by the wet etching process.

For sandblast, the substrate is masked using a 100 μm thick negative dry film resist (Tokyo Ohka Kogyo, BF410). Sandblast was performed using alumina-based abrasive compound with an average diameter of 18 μm. Figure 4 (b) shows a 80 μm deep cavity fabricated by the sandblast process.

3.3 Bonding Hermetic bonding of the first and second layers is necessary to form the reference pressure cavity. There can

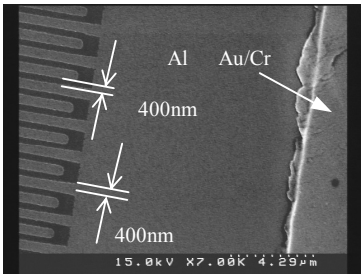

Fig. 3. Fabricated interdigital transducer

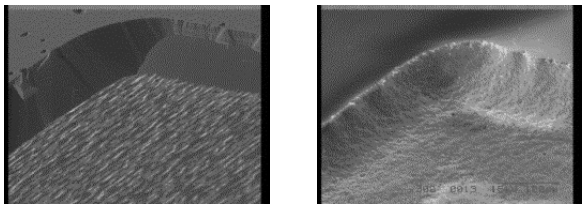
(a) Wet etching (b) Sandblast

Fig. 4. Reference pressure cavity

be several methods of hermetic bonding of $LiNbO_3$: direct bonding in air and vacuum, solder bonding and glass frit bonding. In this study, we selected direct bonding in air, because it needs no intermediate layer, which can degrade the temperature characteristic of the sensor. Note that $LiNbO_3$ was also used as the second layer material, because it has anisotropy in the coefficient of thermal expansion, making it difficult to bond with other material at raised temperature.

For direct bonding, the flatness, smoothness and cleanness of bonding surfaces are quite important. We confirmed that it was possible to directly bond two bare $LiNbO_3$ wafers after careful cleaning. However, the wafer which was etched to make the cavities could not be bonded with a bare wafer. We measured the surface roughness of the etched wafer using an atomic force microscope (AFM). As shown in Table 2, the surface on which the Au/Cr mask was once formed and removed is rougher than that of the bare wafer. This result suggests that Au/Cr sputtering at 170 °C might cause the surface roughness.

The second layer fabricated by sandblast was directly bonded with the first layer. Sandblast was done using the dry film resist, which does not damage the surface, as shown in Table 2. After the first and second layers were pre-bonded in air at room temperature, they were annealed in vacuum at 400 °C for 2 h to increase the bonding strength. Finally, the sensor with the hermetically-sealed reference pressure cavity was successfully obtained.

4. Evaluation

4.1 Experimental Setup The sample was set in a pressure chamber, which is connected to a compressed nitrogen cylinder through a pressure regulator. A strain gage type pressure sensor (Kyowa Electronic Instruments, PG-10KU) was set in the pressure chamber as a reference. The response of the SAW pressure sensor was measured as a form of phase changes using an interrogation unit (Siemens, SOFIS reader)[7]. The antennas used in this study are commercially-available ones (Huber and Suhner), whose specifications are shown in Table 3. The distance between the antennas of the sensor and the interrogation unit was kept at 20 cm.

4.2 Temperature Sensitivity At first, we measured the relationship between temperature and the phase changes of the SAW pressure sensor for temperature compensation. The temperature-dependant formulation of time delay τ is represented as

$$\tau(\Delta T) = \tau_0(1 + TCD \cdot \Delta T), \quad \cdots\cdots(4)$$

where τ_0 is the initial time delay, ΔT is temperature change, and TCD is the temperature coefficient of delay. The sensitivity for a given time delay is

$$S_\tau = \frac{\partial \tau}{\partial T} = \tau_0 TCD . \quad \cdots\cdots(5)$$

The phase φ is related to the time delay as $\varphi = 2\pi f\tau$, where the frequency f corresponds to the center frequency of 2446 MHz. From Equation (5), the temperature sensitivity of the phase is represented as

$$S_\varphi = \frac{\partial \varphi}{\partial T} = 2\pi f \tau_0 TCD . \quad \cdots\cdots(6)$$

The SAW pressure sensor and a K-type thermocouple as a temperature reference were set together on a hotplate. The thermocouple was set just beside the sensor, and this setup was covered with an aluminum foil to ensure that the temperatures of the sensor and the thermocouple were equal. The hotplate was once heated, and then naturally cooled. During the cooling process from 38 °C to 25 °C, the sensor was evaluated. Figure 5 shows the relationship between the temperature and the normalized phase change of each delay line. Measured TCD is 84.5 ppm/K in average, which is slightly larger than the theoretically value for 128° YX $LiNbO_3$ (72 ppm/K)[10]. TCD measured in this study is almost identical to that measured in the previous study[13]. The difference between the experimental and theoretical values could originate from the chip mounting with epoxy.

4.3 Pressure Sensitivity The relationship between applied pressure and the phase change of the SAW pressure sensor was measured using the setup described in Section 4.1. The pressure chamber was once pressurized, and then slowly depressurized. In the depressurization from 280 kPa to 20 kPa, each reflector response was measured. Figure 6 shows the relationship between the pressure and the normalized phase change of each delay line in time domain. The change of φ_4 corresponding to the reflector 4 is slightly larger than that of other phases. This difference suggests that the pressure change only influences φ_4.

The change of φ_1, φ_2 and φ_3 are almost identical after normalized by the length of each delay line, suggesting that they

Table 2. Surface roughness of bare and processed wafers

Wafer status	Bare	Wet-etched	Sandblasted
R_a (nm)	0.5~1.0	2.0~6.0	0.6~1.5
Z_{max} (nm)	22	48	18

Table 3. Specification of the antennas

	Type	Polarization	Freq. range	Gain
Interrogation unit	Planar	LHCP*	2300~2500 MHz	14.5 dBi
SAW sensor	Planar	LHCP*	2300~2500 MHz	8.5 dBi

*Left-hand circular polarized

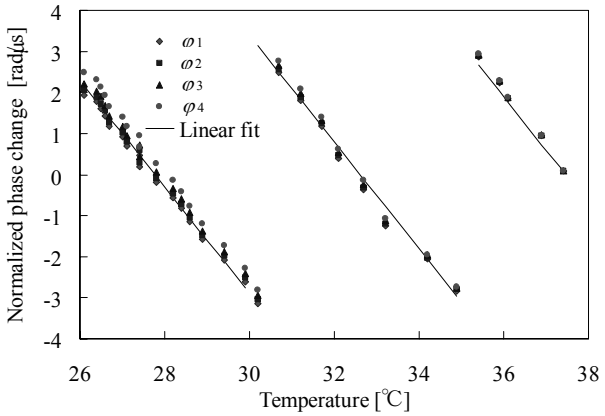

Fig. 5. Normalized phase change of each delay line as a function of temperature change; φ_n represents the phase change for the reflector n

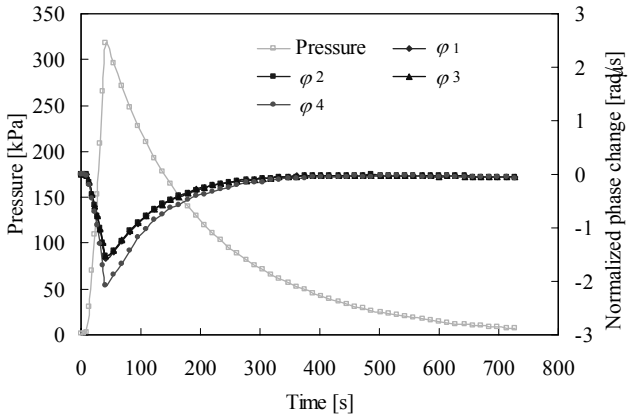

Fig. 6. Normalized phase change of each delay line with respect to pressure change in time domain

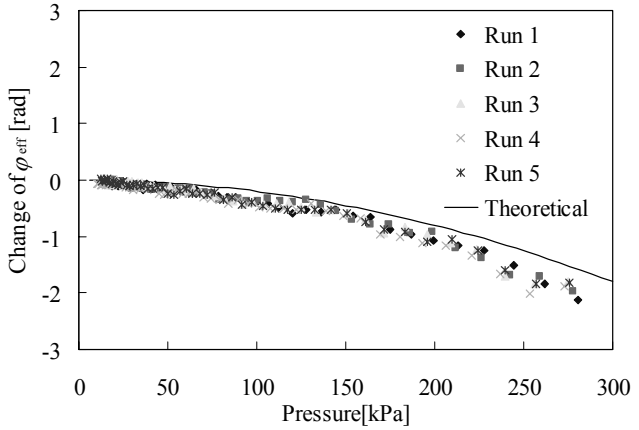

Fig. 7. Change of the effective phase φ_{eff} by pressure change

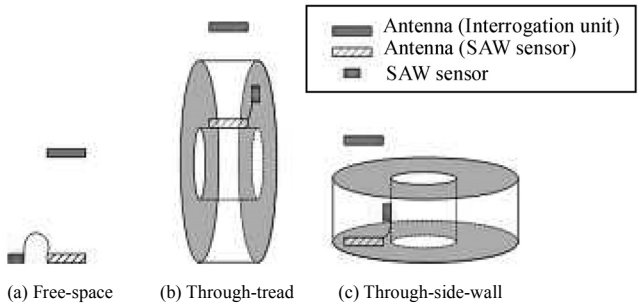

Fig. 8. Configurations of the antennas and the SAW sensor for SNR evaluation experiment in a tire

Table 4. SNR measurement results

	(a) Free-space	(b) Through-tread	(c) Through-side -wall
SNR	10.7±1.0dB	10.0±1.0 dB	11.9±1.0 dB

resulted from temperature change. From the result described in the previous section, the measured phase changes correspond to a temperature change of ca. 1.2 °C, which might occur due to the pressurization and depressurization.

The pressure is estimated with temperature compensation using the following effective phase:

$$\varphi_{\text{eff}} = \varphi_4 - \varphi_3 - \frac{d-c}{b-a}(\varphi_2 - \varphi_1), \quad \cdots\cdots (7)$$

where a, b, c and d are the length of the delay lines, as shown in Figure 2. Figure 7 shows the effective phase φ_{eff} as a function of the pressure for five runs. The result shows good repeatability, suggesting pressure measurement based φ_{eff} is feasible. The obtained φ_{eff} is nearly similar to the theoretical estimation using Equations (1) to (3), which is also shown in Figure 7.

The phase repeats every 2π. Therefore, a single value cannot be determined, if the measurement range corresponds to phase change larger than 2π. This problem is referred as "phase ambiguity", but it can be solved by a multi-step evaluation scheme using time delays and phase changes[6].

4.4 SNR Evaluation Assuming that the SAW pressure sensor is used in a tire, the influence of the tire on the wireless interrogation of the sensor was investigated. We used an automobile tire (185/70 14 inch), a SAW strain sensor, which is similar to the first layer of the SAW pressure sensor and the interrogation system described in Section 4.1.

The signal-to-noise ratio (SNR) of the sensor response was measured in the following three cases illustrated in Figure 8: (a) free-space communication, (b) through-tread communication and (c) through-side-wall communication. The distance between two antennas was approximately 20 cm in each case.

The measured SNR for each case is shown in Table 4. Against expectation, SNR for the through-side-wall communication is higher than that for the free-space communication. The metal wires in the tire might have a positive effect on the SNR. Anyway, the result indicates that tires have little negative influence on wireless communication, at least if they do not rotate.

5. Conclusion

This paper described the design, fabrication and evaluation of the wireless SAW delay line pressure sensor. SAW delay lines operating at 2.45 GHz were fabricated on a 100 μm thick 128° YX $LiNbO_3$ substrate, a part of which was used as a pressure-detective diaphragm. This layer was directly bonded with a 500 μm thick $LiNbO_3$ substrate, in which a reference pressure cavity was fabricated by sandblast.

The fabricated SAW pressure sensor was evaluated in terms of temperature and pressure sensitivity. The measured temperature coefficient of time delay is 84.5 ppm/K in average, which is slightly larger than the theoretically value for 128° YX $LiNO_3$ (72 ppm/K), but almost identical to the previous result. The pressure

measurement was successfully demonstrated in the pressure range of 20~280 kPa with good repeatability. The measured pressure sensitivity well agrees with the theoretical one.

Finally, the influence of a tire on the wireless interrogation of the sensor was investigated. The result indicates that automobile tires have little negative influence on wireless communication, at least if they do not rotate.

Acknowledgment

Tohoku University was supported in part by the Strategic Information and Communications R&D Promotion Program (SCOPE) from the Ministry of General Affairs, Japan (No. 062302002).

(Manuscript received Aug. 31, 2007, revised Jun. 9, 2008)

References

(1) A. Pohl : "A review of wireless SAW sensors", IEEE Trans. Ultrason., Ferroelect., Freq. Contr., Vol.47, No.2, pp.317-332 (2000)
(2) L. Reindl, G. Scholl, T. Ostertag, C. C. W. Ruppel, W.-E. Bulst, and F. Seifert : "SAW Devices as Wireless Passive Sensors", Proc. IEEE Ultrason. Symp., pp.363-367 (1996)
(3) A. Pohl, G. O. Stermayer, L. Reindl, and F. Seifert : "Monitoring the Tire Pressure at Cars Using Passive SAW Sensors", Proc. IEEE Ultrason. Symp., pp.471-474 (1997)
(4) B. Dixon, V. Kalinin, J. Beckley, and R. Lohr : "A Second Generation In-car Tire pressure Monitoring System Based on Wireless Passive SAW Sensors", Proc. IEEE Freq. Cont. Symp., pp.374-380 (2006)
(5) A. J. Slobodnik : "Surface Acoustic Waves and SAW Material", Proc. IEEE, Vol.64, No.5, pp.581-595 (1976)
(6) J. H. Kuypers, D. A. Eisele, L. M. Reindl, S. Tanaka, and M. Esashi : "Passive 2.45 GHz TDMA-based Multi-Sensor Wireless Temperature Monitoring System: Results and Design Considerations", Proc. IEEE Ultrason. Symp., pp.1453-1458 (2006)
(7) J. H. Kuypers : "MEMS-based SAW devices for wireless sensing", Ph.D thesis, Department of Nanomechanices, Tohoku University (2007)
(8) W. Wang, K. Lee, I. Woo, I. Park, and S. Yang : "Novel SAW-based sensor on 41° YX-$LiNbO_3$ for wireless pressure measurement", Proc. Asia-Pacific Conference of Transducers and Micro-Nano Technology (2006)
(9) A. L. Nalamar and M. Epstein : "Strain Effects in SAW Devices", Proc. IEEE, Vol.64, No.5, pp.613-615 (1976)
(10) "Elastic Wave Device Technology Handbook", Ohm-sha, Japan (1991)
(11) "Mechanical Engineering Handbook A4", The Japan Society of Mechanical Engineers (1984)
(12) A. Randles, S. Tanaka, B. Pokines, and M. Esashi : "Bulk-micromachined lithium niobate sensor and actuator for harsh environments", Proc. Transducers, pp.1380-1383 (2005)
(13) J. H. Kuypers, D. A. Eisele, L. M. Reindl, S. Tanaka, and M. Esashi : "2.45GHz Passive Wireless Temperature Monitoring System Featuring Parallel Sensor Interrogation and Resolution Evaluation", Proc. IEEE Sensors, pp.773-776 (2006)

Shuhei Hashimoto

(Non-member) received B.E degree in Aerospace Engineering in 2003 from Nagoya University and M.E degree in mechanical and control engineering in 2005 from Tokyo Institute of Technology. He has been working on the evaluation of mechanical properties of various automobile sensors at Measurement Engineering Department of Nissan Motor Company. He developed MEMS-based SAW sensors at Tohoku University from 2006 to 2007.

Jan H. Kuypers

(Non-member) received Dipl.-Ing. degree from the Department of Microsystem Technology IMTEK at the University of Freiburg, Germany in 2004, and Ph.D. degree in Nanomechanics from Tohoku University, Japan in 2007. He has been working on the evaluation of mechanical properties of MEMS thin films, deposition of aluminum nitride thin films, FBAR, SMR, modeling of SAW devices, wireless SAW sensors, MEMS based SAW devices, and wafer level packaging. He is the author of the K-model, a higher order Green's function based simulation model for SAW devices. He was awarded the best Student Paper at the IEEE Ultrasonics Symposium 2007. He is member of the IEEE, Ultrasonics, Ferroelectrics, and Frequency Control (UFFC) society and the Microwave Theory and Techniques society. Since 2007, he is a member of the technical program committee of the UFFC. He is currently working as a research specialist at the Berkeley Sensor and Actuator Center (BSAC) at the University of California.

Shuji Tanaka

(Member) received B.E., M.E. and Dr.E. degrees all in mechanical engineering from The University of Tokyo in 1994, 1996 and 1999, respectively. From 1996 to 1999, he was Research Fellow of the Japan Society for the Promotion of Science. He was Research Associate at Department of Mechatronics and Precision Engineering, Tohoku University from 1999 to 2001, Assistant Professor from 2001 to 2003. He is currently Associate Professor in Department of Nanomechanics, Tohoku University. He was also Fellow of Center for Research and Development Strategy, Japan Science and Technology Agency from 2004 to 2006, and is currently Selected Fellow. His research interests include Power MEMS, RF MEMS, SiC MEMS and miniaturized gas turbine generators.

Masayoshi Esashi

(Member) received B.E. and Dr.E. degrees in electronic engineering from Tohoku University in 1971 and 1976, respectively. He was Research Associate in Department of Electronic Engineering, Tohoku University from 1976 to 1981, and Associate Professor from 1981 to 1990. He was Professor in Department of Mechatronics and Precision Engineering, Tohoku University from 1990 to 1998, and moved to New Industry Creation Hatchery Center, Tohoku University until 2004. He is currently President of Micro Nanomaching Research and Education Center, Tohoku University as well as Professor in Department of Nanomechanics, Tohoku University. His research interests include MEMS, integrated sensors, micromachining technology and packaging.